DENTAL MATERIALS 35 (2019) 871–882

Available online at www.sciencedirect.com

ScienceDirect

journal homepage: www.intl.elsevierhealth.com/journals/dema

Factors influencing development of residual stresses during crystallization firing in a novel lithium silicate glass-ceramic

Michael Wendler[a,*], *Renan Belli*[b], *Ulrich Lohbauer*[b]

[a] *Department of Restorative Dentistry, Faculty of Dentistry, Universidad de Concepción, Concepción, Chile*
[b] *Friedrich-Alexander-Universität Erlangen-Nürnberg (FAU), Zahnklinik 1 – Zahnerhaltung und Parodontologie, Forschungslabor für dentale Biomaterialien, Erlangen, Germany*

ARTICLE INFO

Article history:
Received 20 January 2019
Received in revised form
4 March 2019
Accepted 6 March 2019

Keywords:
Glass-ceramic
Crystallization
Residual stress
Lithium silicate
Firing tray
Cooling protocol
Lifetime

ABSTRACT

Objective. Development of residual stresses is a potential source of premature fractures in glassy materials, being of special interest in novel lithium silicate glass-ceramics that require a crystallization firing to achieve their final mechanical properties. The aim of this work was to assess the influence of various firing tray systems and the application of different cooling protocols on the development of residual stresses in Suprinity PC crowns. Their effect on the in vitro lifetime of the restorations was also studied.

Methods. Thirty crowns were milled out of Suprinity PC blocks and crystallized using one of five different commercial firing tray systems (n = 6). Samples in each group were cooled following a fast (FC = 5.5 °C/s), a slow (SC = 0.4 °C/s) or the manufacturer's reference cooling (REF). Obtained crowns were sagittally or transversally sectioned and the magnitude and distribution of residual stresses was determined using the light birefringence method. Extra crowns of three of the subgroups (n = 8) were produced and submitted to chewing simulation for 10^6 cycles or until fracture ensued.

Results. Average residual stresses ranged between 0 and 1.5 MPa (peaks of 5 MPa). Highest stress magnitudes were observed at the support areas of groups using firing pins, leading to thermal cracks in FC samples and premature failures in the REF subgroup. The use of fibrous pads and firing pastes limited the development of residual stresses, whereas application of SC regimes extended the lifetime of the restorations.

Significance. Development of residual stresses during crystallization firing in lithium silicate glass-ceramics results critical for their mechanical performance and should be therefore avoided by ensuring a homogenous cooling of the structures.

* *Corresponding author at*: Department of Restorative Dentistry, Faculty of Dentistry, Universidad de Concepción, Roosevelt 1550, 4070369 Concepción, Chile.
E-mail address: mwendler@udec.cl (M. Wendler).
https://doi.org/10.1016/j.dental.2019.03.002

1. Introduction

The fast expansion of computer aided design and manufacturing (CAD/CAM) technologies in dentistry has given rise to the development of a broad variety of new ceramic and polymeric materials, seeking for unexploded market niches. Following the success of leucite and feldspar reinforced glasses for the production of monolithic restorations in the anterior region of the mouth, the introduction of lithium disilicate glass-ceramics (LS_2) as a reliable replacement for metal alloys in the posterior region constituted a milestone in the development of metal-free restorations in dentistry [1]. The unique microstructure of this material [2] enables the combination of strong mechanical properties (strength and fracture toughness) without compromising its high translucency.

Recently, a new glass-ceramic marketed as zirconia-reinforced lithium silicate was introduced as an alternative to LS_2 restorations in high load bearing areas, such as molar crowns and implant abutments. Starting from a SiO_2–Li_2O–ZrO_2–P_2O_5 multicomponent glass, three main crystalline phases (namely lithium metasilicate, Li_2SiO_3; lithum disilicate, $Li_2Si_2O_5$; and lithium orthophosphate, Li_3PO_4) are formed during a two-stage crystallization process of the material [3]. The larger amount of ZrO_2 incorporated (up to 12 vol%) restricts the growth of the crystals by incrementing the number of crystallization nuclei and increasing the viscosity of the glass [4]. In addition, ZrO_2 seems to favor the crystallization of Li_2SiO_3 at the expenses of $Li_2Si_2O_5$, leading to a final glass-ceramic consisting of round and slightly elongated Li_2SiO_3 and $Li_2Si_2O_5$ crystals (0.5–1 μm in length) and nanometric Li_3PO_4 granule-shaped crystals [5]. The smaller size of the crystals compared to LS_2 is assumed to increase the translucency of the material, while the ZrO_2 dispersed in the glass matrix has been claimed to increase its mechanical resistance to fracture and wear [6–9].

In order to ease the machining step, the company Vita Zahnfabrik commercializes its lithium silicate/ disilicate material Suprinity PC in a meta-sintered stage, displaying a lower hardness, but also reduced mechanical properties. Once the restoration is milled, a so-called crystallization firing has to be conducted in order to allow the full growth of the Li_2SiO_3, $Li_2Si_2O_5$ and Li_3PO_4 phases at the expense of the glassy phase [3, 9] and thus, achieve its final optical and mechanical properties. Further improvement in strength is expected by crack healing of defects and grinding damage introduced during the machining step. On the other hand, the presence of different phases in the material gives rise to the development of residual stresses upon cooling from crystallization temperatures, mainly due to thermal and elastic mismatches between the glassy matrix and the precipitates [10]. This takes place at a microscopic level and has shown to be beneficial in glass-ceramics if the coefficient of thermal expansion (CTE) of the crystals exceeds that of the glass matrix and hence compressive residual stresses develop around the former [11]. In addition to these microscopic stresses, macroscopic residual stress can develop in glass-ceramic materials as a consequence of the firing conditions [12]. In the case of layered structures, a large discrepancy in the CTE between the substrate and the veneer layer has shown to be responsible for residual stress development at the interface of both materials [13,14]. This kind of residual stress can also arise during crystallization firing of monolithic glass-ceramics if an adequate isolation from the supporting tray or refractory material is not ensured, allowing a partial or total fusion between materials. On the other hand, occurrence of thermal gradients, mainly due to a sufficiently fast drop in the temperature during the cooling phase, causes an inhomogeneous solidification of the material and, accordingly, development of residual stresses across the structure [15]. The presence of macroscopic stresses has shown to influence the propagation of cracks [14,16], by limiting (compressive stresses) or favoring (tensile stresses) their growth and thus, affecting the mechanical behavior of the restoration. This phenomenon has been also observed in lithia based glass-ceramics [17], where the presence of compressive residual stresses in the surface limited the growth of indentation cracks. The real impact of these stresses on LS2, however, has been recently questioned [18], as their low magnitude seemed to be unable to affect the mechanical behavior of the glass-ceramic.

The crystallization firing of Suprinity PC is usually conducted at the dental laboratory by the technician or, if chairside devices are used, at the dental office by the dentist or its assistant. Hence, the firing conditions are ultimately set here, following (or not) the manufacturer's instructions. This opens the door to external factors to influence the crystallization process and, in this manner, the residual stress state in the structures. Therefore, the goal of the present study was to assess the influence of some of these variables, namely the use of different firing tray systems and the application of fast or slow cooling protocols, on the magnitude and distribution of macroscopic residual stresses in Suprinity PC monolithic crowns. The null hypothesis tested was that the firing conditions would not influence the distribution and magnitude of residual stresses in the crowns. The effect of the generated residual stresses on the in vitro lifetime of the restorations was also studied.

2. Material and methods

2.1. Material

A highly translucent shade (0M1-HT) of the lithium silicate glass-ceramic Suprinity PC (Vita Zahnfabrik, Bad Säckingen, Germany) was selected for this study, following pilot experiments to determine its suitability for the light birefringence method. The LS14 CAD/CAM blocks (LOT 59840) were received in a pre-crystallized ("blue") state and used to machine the samples.

2.2. Measurement of the coefficient of photoelasticity (C_{el})

The coefficient of photoelasticity of the material was determined according to the method described by Belli et al. [13]. Briefly, 3 disc-shaped samples (thickness, $t = 2.30$ mm; diameter, $D = 14$ mm) were obtained from an LS14 Suprinity PC block and subsequently crystallized. Following fine polishing, the discs were annealed at 650 °C for 5 min and then slowly cooled

with the furnace closed until 200 °C were reached. Absence of residual stresses in the discs was controlled with a real time automatic polarimeter (StrainScope, ilis GmbH, Erlangen, Germany). The samples were submitted to a diametral tensile test with a step-wise loading in 20 N intervals up to 500 N. Simultaneous transillumination with the polarized light beam of the StrainScope allowed measurement of the optical retardation at each loading step. The diametral tensile stress was then calculated using the applied load (P) and the specimen dimensions according to:

$$\sigma = 2P/\pi Dt \quad (1)$$

Obtained stress data was then plotted against the normalized optical retardation at each stress level, with the resulting slope of the curve corresponding to the C_{el} of the material. An average of 8.09 (±0.05) 1/TPa was calculated from the 3 tested samples and further use to determine the residual stress state in the crowns.

2.3. CAD/CAM manufacturing of crowns and crystallization protocols

A first molar crown was digitally designed using a CAD software (Modellier, ZirkonZahn, Bruneck, Italy) and the generated file was used to mill crowns out of Suprinity PC CAD/CAM blocks in the pre-crystallized ("blue") state using a Sirona inLab MC XL (Sirona, Bensheim, Germany) milling unit. The obtained structures were then ultrasonically cleaned and divided into five groups according to the firing tray system used for the crystallization process (as depicted in Fig. 1), which was conducted in a Vacumat 4000 (Vita Zahnfabrik) furnace. Crystallization firing followed manufacturer recommendations (i.e. heating rate of 55 °C/min and a holding time at 840 °C of 8.00 min). Each group was then subdivided into three different cooling protocols, as described in Table 1. During the cooling step, the furnace door was kept closed until the desired temperature inside the oven was reached, whereupon the furnace completely opened exposing the crown to the ambient temperature. The reference group (REF, furnace door opened at 680 °C) followed the current crystallization protocol of the manufacturer for this material. Temperature profiles during the cooling process for this group, as well as for the fast cooling (FC, furnace opening at 840 °C) and the slow cooling (SC, at 550 °C), were measured by means of a N-type thermocouple (Omega Engineering, Manchester, UK) placed inside the crown lumen during the crystallization process.

2.4. Light birefringence measurement in the crowns

Six crowns were milled for each firing tray system (groups 1–5) and randomly assigned in pairs to one of the three cooling protocols. After crystallization, both crowns in each subgroup were sectioned using a 0.3 mm thick diamond blade mounted in a low speed saw (IsoMet, Buehler, Lake Bluff, IL, USA) under constant water irrigation. Each crown was cut following a different orientation, sagittal or transversal to its main axis (Fig. 2), to obtain respectively six sagittal (average thickness of 1.00 ± 0.1 mm) and four transversal slices. The thicknesses of the latter varied between 1.2 ± 0.1 mm in the cervical region of the crown and 1.75 ± 0.1 mm in the mid-coronal section, in order to preserve the inner-side area of the crown where the support pin of groups 1–3 contacted the material.

An automatic polarimeter with a spatial resolution of 11 μm/px was used to conduct the stress birefringence measurement in the crowns (StrainMatic M4/120.33, ilis GmbH). The obtained slices were positioned flat in the machine keeping a constant orientation towards the light beam, in order to facilitate inter-specimen comparison. During each measurement, the rotation angle (α) of the light beam was acquired and used to calculate the light retardation (δ) using [19]:

$$\delta = \alpha\lambda/180^{\circ} \quad (2)$$

with the wavelength of the light source (λ) at 593 nm. The C_{el} of the material was then used to calculate the residual stresses (σ_{res}) in the slices, normalized by its thickness (t), according to [20]:

$$\sigma_{res} = \delta/t \cdot C_{el} \quad (3)$$

The obtained data was then processed using the StrainAnalyzer software (v. 2015.190, ilis GmbH) in order to create image files where color scales for the residual stress distribution were adjusted.

2.5. Chewing simulation

Twenty-four additional crowns were fabricated and crystallized using one of the three following protocols (n = 8):

- REF cooling using the dark ceramic tray and pin (as in group 2)
- REF cooling using the honeycomb tray and the fibrous pad (as in group 4)
- SC using the honeycomb tray and the fibrous pad (as in group 4)

The intaglio surface of the obtained crowns was etched with 5% hydrofluoric acid (Ceramic Etch, Vita Zahnfabrik) for 20 s and then rinsed with water spray. After ultrasonic cleaning in ethanol for 3 min, a silane-coupling agent (ESPE Sil, 3 M ESPE, Seefeld, Germany) was applied onto the etched surface. The digital model of the crown was used to machine 24 brass holders, which recreated the original tooth preparation or stump (Fig. 3A). The surface of the brass stumps was then sandblasted with 50 μm glass-beads at 2 bar pressure and subsequently silanized. Crowns were luted onto the brass stumps using a dual-cure resin cement (RelyX Unicem 2, 3M ESPE), light polymerized from different directions for 80 s and then stored for 24 h in distilled water at 37 °C.

Specimens were then mounted in an eight-chamber chewing simulator (CS-4.8, SD Mechatronik, Feldkirchen, Germany) and submitted to axial cyclic contact fatigue against a steel indenter, as shown in Fig. 3B. Each crown received a periodic load of 80 N at a 1.5 Hz frequency. Testing was conducted in distilled water at 37 °C for 10^6 cycles or until fracture ensued. Samples were checked regularly by partially removing the water from the testing chamber and transilluminating the glass-ceramic crown with a blue-light lamp to determine the

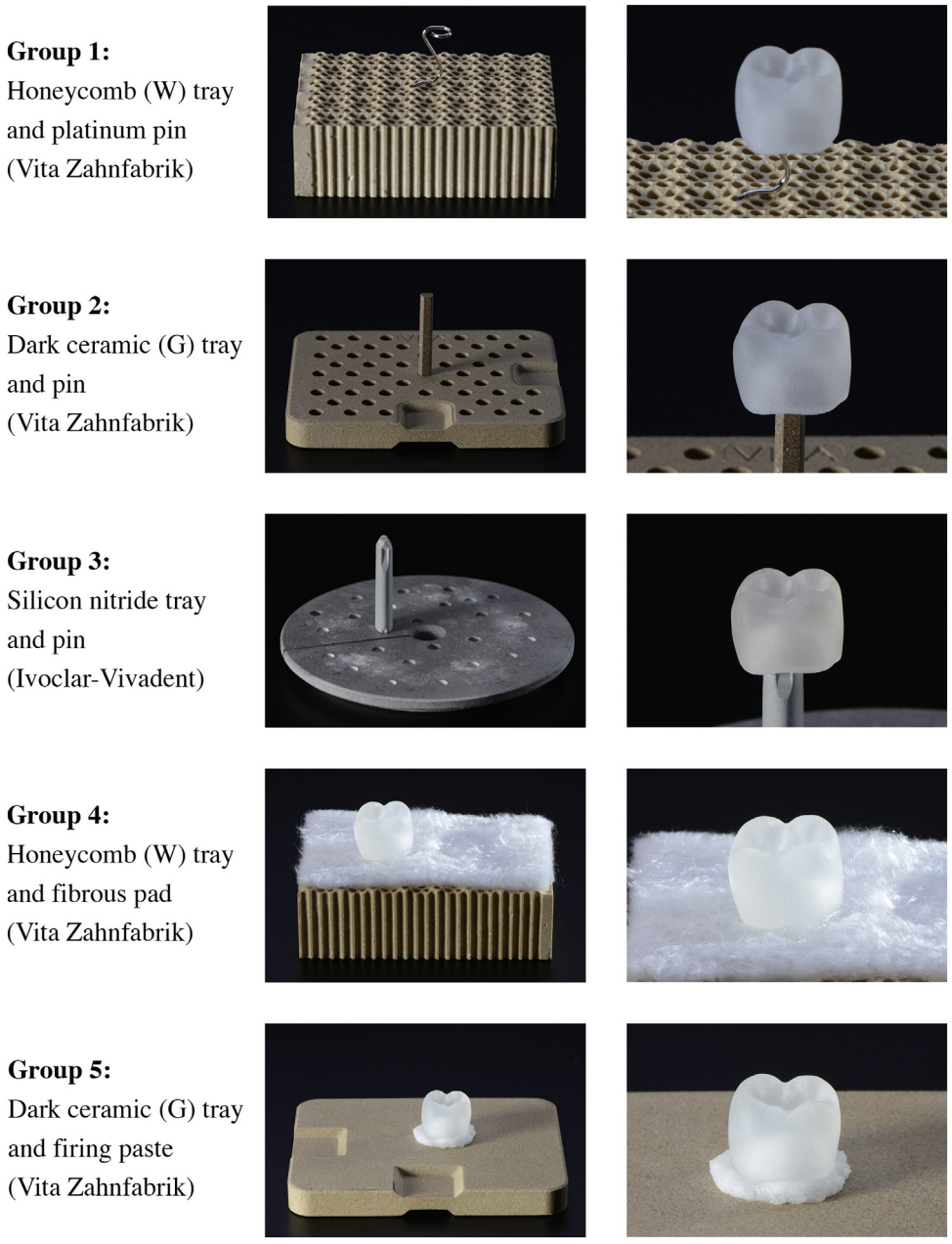

Fig. 1 – Support trays systems used for the crystallization firing of the different groups in this study. Samples of groups 1–3 were placed directly in contact with the firing pin. The lumen of the crowns of group 5 was completely filled with the firing paste, whereas samples in group 4 were placed over the fibrous pad, without any internal filling.

Table 1 – Crystallization protocols.

Group	Pre-drying		Crystallization			Cooling
	Temp. (°C)	Hold (min)	Heat. Rate (°C/min)	Temp. (°C)[a]	Hold (min)	Furnace closed up to (°C)
Slow Cooling (SC)	400	4.00	55	840	8.00	550
Reference (REF)	400	4.00	55	840	8.00	680
Fast Cooling (FC)	400	4.00	55	840	8.00	840

[a] According to the manufacturer instructions. Samples of group 4 were crystallized at 850° for 8.00 min in order to compensate the isolating effect of the fibrous pad.

presence of cracks in the material (Fig. 3C). These inspections were carried out after every 10^2 cycles until 10^4 cycles were reached and then after every 10^4 cycles until testing was completed.

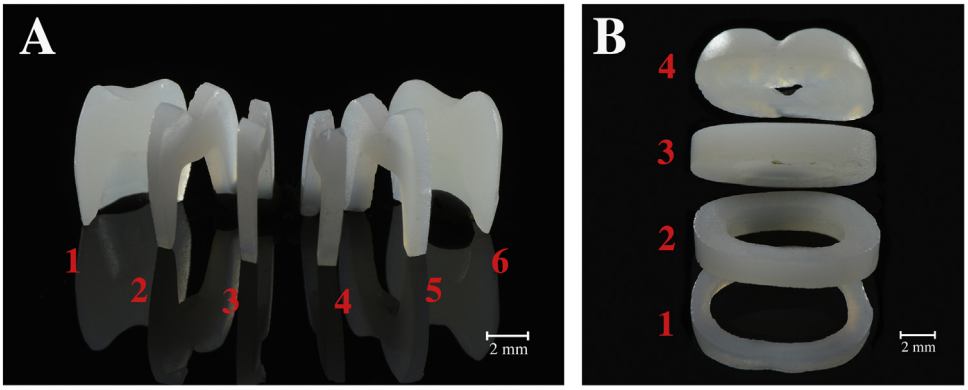

Fig. 2 – Sample sectioning orientations in each subgroup. In (A), 6 sagittal sections with an average thickness of 1 mm ± 0.1 mm were cut parallel to the crown's main axis. Only slices 2–5 were used for the light birefringence measurement. In (B), the four transversal slices had different thicknesses, varying between 1.2 mm for slice 1 and 1.7 mm for slice 3. Slice 4 was not measured with the light birefringence method.

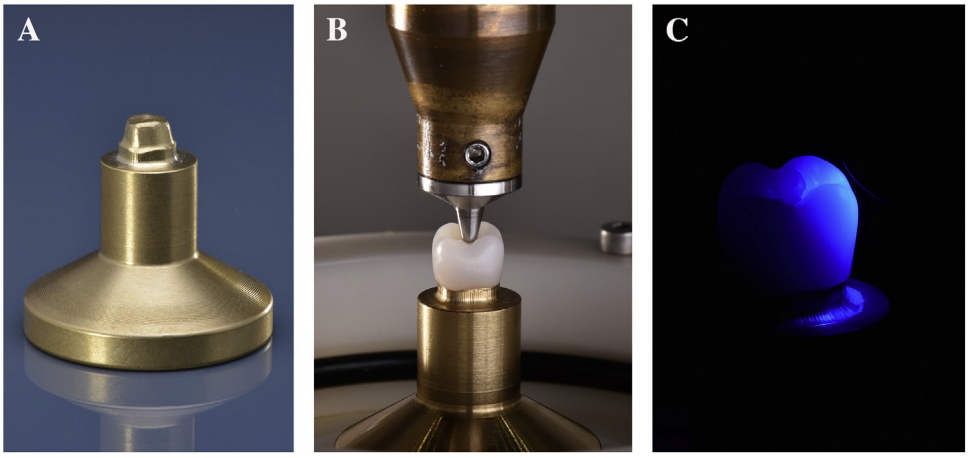

Fig. 3 – Test set-up used for the chewing simulation. (A) Brass replica of the original tooth preparation. (B) Steel indenter contacting the occlusal surface between the cusps of the crown. This position was standardized for all samples and was kept constant upon completion of the test. (C) Transillumination of the crowns with a blue-light lamp in order to reveal the presence of cracks in the glass-ceramic. Water was removed from the testing chamber prior to examination.

3. Results and discussion

3.1. *Residual stresses in the crowns*

Precise quantification of residual stress magnitudes in geometrically complex structures, as those studied here, is still an unsolved issue in the literature [12]. Most approaches using indirect methods, such as the effect of residual stresses on the propagation of cracks from sharp indentations [14,16,21] or its influence on the strength degradation of the component [22,23], face limitations related to the intrinsic mechanical properties of the material, as well as to overlapping of the stress fields during the test. Finite element analyses, on the other hand, provide a good approach to study this problem, although their estimations are limited by the difficulties encountered in the simulation of the viscoelastic behavior of the glass-ceramic through the glass transition (T_g) range. The light birefringence method used here has shown promising results in previous works on glassy veneers [13,24,25], being able to characterize stresses locked inside thin layers of these materials. Its principle, based on the effect of residual stresses on the phase delay of the two component waves of a polarized light beam passing through the sample [19], allows a theoretically non-destructive assessment of the residual stress state. However, two important considerations have to be taken into account for its application. In first place, materials submitted to this technique need to have a high translucency, allowing an adequate passage of light through the specimen. In the present study, preliminary tests were conducted in order to determine the shade of the material that met best this criterion, permitting neat observation of residual stresses even if they occurred at low magnitudes. The second requirement is related to the flatness and thickness of the samples, as an important reduction in the accuracy of the measurement is observed in non-planar or excessively thick specimens. This is mainly due to the superposition of residual stresses in the sample and the presence of round edges (e.g. cusps areas), which hamper a straight propagation of the light. Therefore,

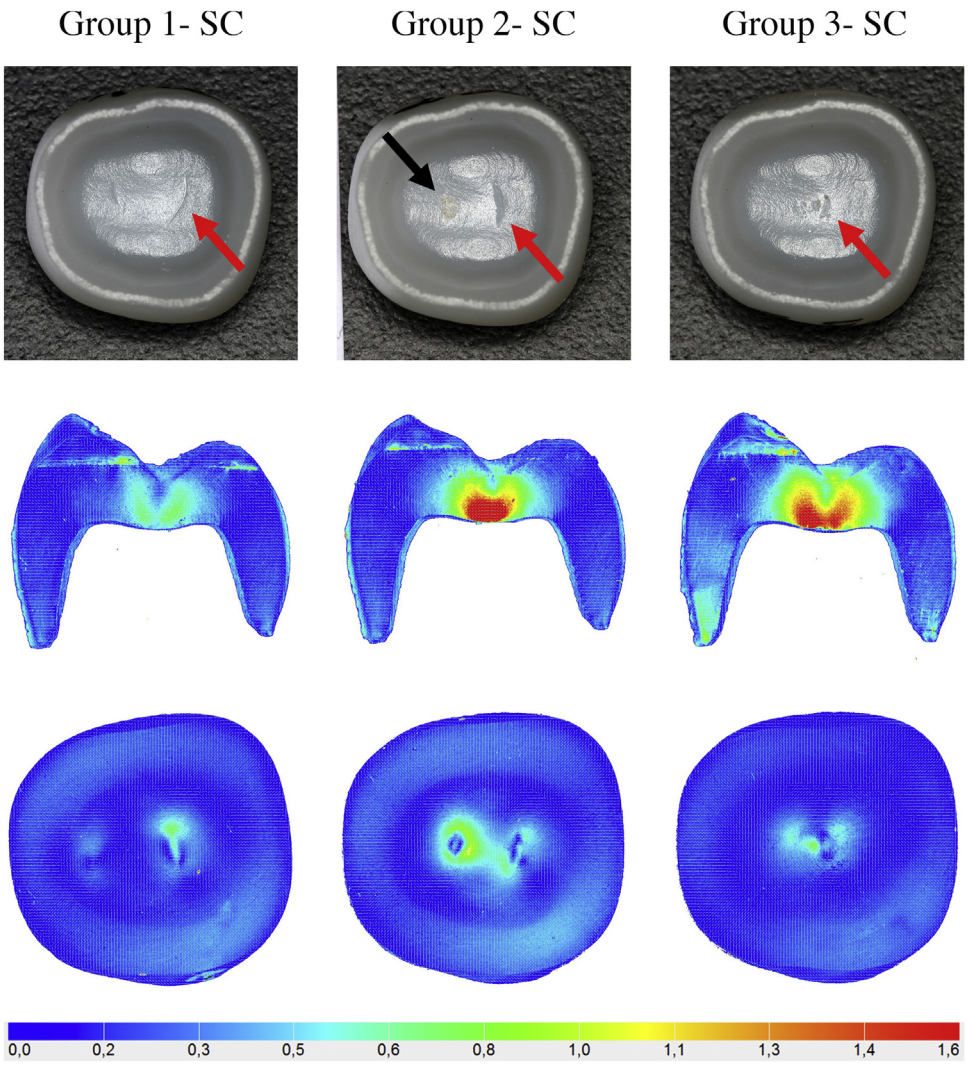

Fig. 4 – Intaglio appearance and light birefringence results (sagittal and transversal slices 3) of the slow cooled crowns of groups 1–3. As indicated by the red arrows, the support firing pins left an impression in the intaglio surface of the crowns. An increased magnitude of residual stresses was observed around this area in groups 2 and 3, especially for the sagittal sections. The platinum pin used in group 1 left a narrower impression in the material and, consequently, less residual stress developed in the material. The partial fusion of the cordierite pin with the glass-ceramic in group 2 is pointed by the black arrow and corresponds to the higher stress magnitudes measured in the transversal section of this sample. The stress color scale was set here between 0 and 1.6 MPa in order to highlight the distribution of the residual stresses. (For interpretation of the references to colour in the text, the reader is referred to the web version of this article.)

complex structures (such as the molar crowns studied here) need to be sectioned into thin slices (for this set up to a maximum of 2 mm in thickness) and subsequently flattened in order to restrict the sources of noise during the measurement.

The main limitation of the light birefringence method arises from the undetermined release of elastic stress in the structure during the sectioning procedure, preserving only specific stress components according to the direction of the cut [25]. A way to overcome this issue is to use different sectioning planes (sagittal, transversal), in order to allow a 3D reconstruction of the residual stress state in the structure. Thus, sagittal sections preserve mainly radial stress components, whereas the hoop (or circumferential) stress component can be measured in tangential slices. In the current study, the mean stress magnitudes ranged between 0 and 1.5 MPa, with maximum peaks of 5 MPa. Highest residual stresses concentrated in sagittal slices 3 and 4 around the support area of the platinum pin (group 1) and both ceramic pins (groups 2 and 3). Additionally, high magnitude residual stresses were measured in FC samples, especially inside the third slice. Although these values do not reflect the residual stress state prior to sample sectioning, they provide an idea of its distribution and relative magnitude between cooling protocols, as well as the strong influence of the tray system used on the development of local residual stress. Accordingly, the null hypothesis was rejected.

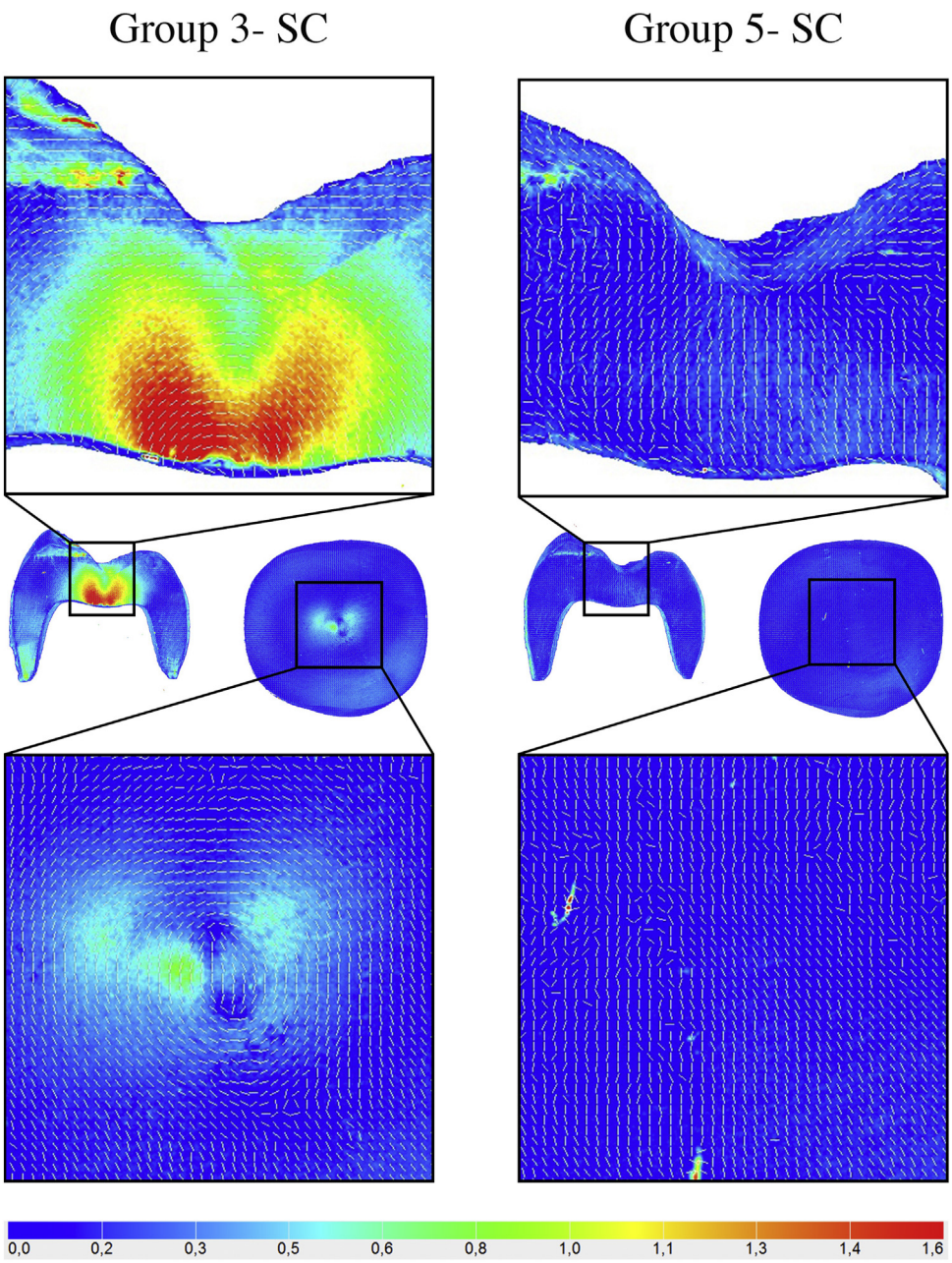

Fig. 5 – Light birefringence results of group 3-SC are compared to those of group 5-SC. The nature of the stress (dashed white lines) is depicted in detail for the third sagittal and transversal slices. Although it is not possible to determine if it is tensile or compressive, its concentric orientation around the support pin in group 3 contrasts with its homogeneous alignment in group 5. A similar tendency was observed in the transversal sections. The magnitude of the stresses was color-coded between 0 and 1.6 MPa.

3.2. *Effect of the firing tray*

The main aim of the current study was to evaluate the influence of crystallization conditions on the development of residual stresses in the crowns. Utilization of firing trays is a common practice in the dental field, aiming to avoid a direct contact of the glass-ceramic with the refractory material of the furnace. In the case of Suprinity PC, no specific tray is indicated for the crystallization process, with a wide spectrum of available alternatives, from firing pastes and fibrous pads to thin metallic wires and ceramic pins [26]. When the latter are used, however, the manufacturer recommends to round the edges of the pins and to cover them with a firing paste or a fibrous path, in order to avoid adhesion to the restorative material [26]. In spite of this indication, it is not unusual for dental technicians to place the restorations in direct contact with the firing pin. Crystallization conducted under these conditions cause a partial fusion of the pin's material with the glass-ceramic during firing, with development of residual stresses during the cooling phase if both materials have

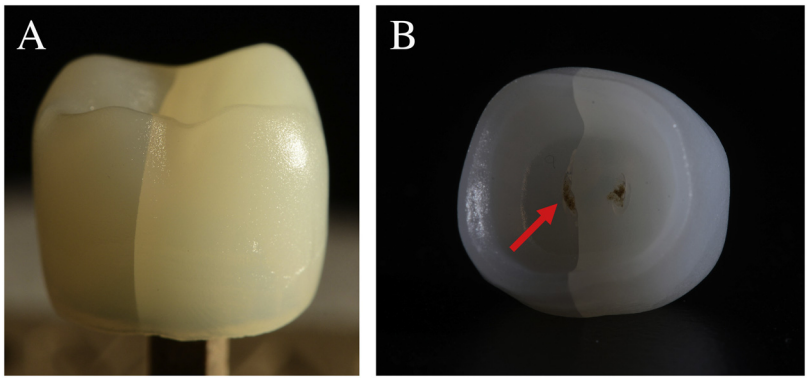

Fig. 6 – Crowns of group 2 that underwent a fast cooling protocol fractured shortly after the furnace door was opened. The crack extended sagittally throughout the structure (A), starting in the vicinity of the support pin, where the cordierite was partially fused to the glass-ceramic, as indicated by the red arrow in (B). (For interpretation of the references to colour in this figure legend, the reader is referred to the web version of this article.)

a sufficiently large difference in their coefficients of thermal expansion. Groups 2 and 3 of this study recreated this worst case scenario, allowing a direct contact of the restorations with, respectively, a cordierite ($Mg_2Al_3[Si_5AlO_{18}]$) and a silicon nitride (Si_3N_4) pin. As depicted in Fig. 4, both ceramic pins left an impression at their support areas in the intaglio surface of the crown (red arrows), with cordierite particles still attached to the glass-ceramic in group 2 (black arrow). In group 1, where a thin platinum pin was used, signs of partial adhesion to the glass-ceramic were also visible (in Fig. 4, the impression left is pointed by the red arrow). These results are interesting, considering that the manufacturer clearly indicates that an isolation paste is not required for its use [26]. No evidence of material attachment or any other sign of contamination on the restoration's intaglio surfaces was observed after crystallization of groups 4 and 5.

In close relation to the observed impressions, concentric residual stresses were detected by the light birefringence method in the glass-ceramic around the support areas of the pins of groups 1–3, as shown in Fig. 4. These stresses had a higher magnitude in the cordierite and silicon nitride groups, as a consequence of the large CTE mismatch between the pin materials and the glass-ceramic. Whereas Suprinity PC displays CTE values around $12 \times 10^{-6}\,K^{-1}$ [26], the refractory materials lie, depending on their phase composition, in the range of 1–$5.7 \times 10^{-6}\,K^{-1}$ for cordierite [27] and between 3–$4 \times 10^{-6}\,K^{-1}$ for silicon nitride [28]. Thus, during the cooling phase the partially fused pin hindered the higher contraction of the glass-ceramic, creating tensile residual stresses around these fixed areas. The magnitude of the stresses decreased in the surrounding material, as contraction upon cooling was allowed away from the contact areas. Still, the residual stress field extended over one half of the crown's thickness. The lower CTE mismatch between the glass-ceramic and the platinum pin ($9 \times 10^{-6}\,K^{-1}$ [29]), in addition to the smaller contact area between both materials (as evidenced by the thin impressions left in the crowns), were responsible for the lower residual stress magnitude observed in group 1 (Fig. 4).

A comparison with the residual stress free structures of group 5-SC is presented in Fig. 5, whose crowns displayed a similar residual stress state as those of group 4-SC (Fig. 7). Under the firing conditions of these latter groups, the glass-ceramic was able to contract homogeneously during cooling. In contrast, the concentric orientation of the stress field in both, sagittal and transversal planes of group 3 denote the inhomogeneous cooling process experienced by the material, with its peak intensities at the contact areas with the pin.

The fast cooled specimens of group 2 experienced the highest thermal stresses, with intensities exceeding the material's fracture resistance. As a consequence, a thermal crack propagated from one of the contact areas with the cordierite pin at the intaglio surface and ran parallel to the bucco-palatal axis of the crown, ultimately reaching both cervical margins (Fig. 6). A complete fractographic analysis of these catastrophic failures was recently conducted by our group [30]. Briefly, the fracture origin was located at the intaglio surface, close to the contact point with the pin. In this area, a reaction zone between both materials was identified using high magnification. A similar fractographic pattern was observed in all failed samples, with fractured surfaces displaying a combination of smooth and sharp twisted fracture planes, which are considered an evidence of steep local stress gradients in the structure [31]. In order to obtain at least two undamaged specimens for the light birefringence measurement, 6 extra crowns of group 2 were submitted to the FC protocol. Nevertheless, only one of them was able to survive the crystallization firing, so that solely transversal sections could be obtained to measure the stress state at the contact area with the pin. Maximum hoop stress values for these slices did not differ from those observed in groups 1 and 3 after fast cooling (with maximum stresses in the range of 4 MPa), although crowns in these groups did not fractured during the cooling phase. Residual stress release due to sample sectioning compromised a "true" determination of the tensions in the material. Alternatively, a rough estimation of the stress magnitudes at failure (σ_f) can be derived from the fracture toughness of the material (1.52 $MPam^{1/2}$, using the B3B-K_{Ic} method [32]) and the size of the critical

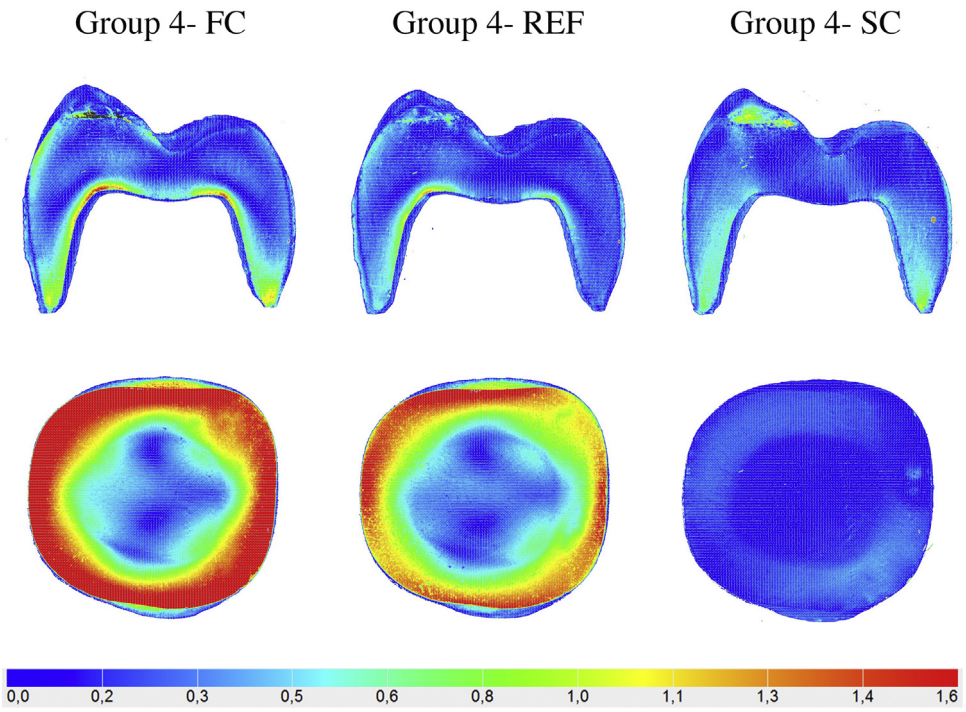

Fig. 7 – Results for the light birefringence measurement of crowns of group 4 after the three different cooling regimes. Stress distributions for the radial component of stress are shown for sagittal slice 3, with no difference among cooling protocols. Residual stresses for the hoop component of stress had a higher magnitude in FC than in REF cooled samples, as shown in the transversal sections. The highest stress magnitudes, having peaks of 3.6 MPa, were measured at the outer rim of FC samples. In contrast, no residual stresses were observed for SC samples. The stress color scale was set between 0 and 1.6 MPa in order to highlight the distribution of the residual stresses.

defect, a, obtained from the fractographic analysis (which had semielliptical shapes and sizes varying between 50 and 80 μm [30]). By solving the Griffith-Irwin relation for σ_f:–

$$K_{Ic} = Y\sigma_f\sqrt{\pi a} \quad (4)$$

with a geometric factor $Y = 0.75$, the critical stresses for fracture initiation would have ranged between 128 and 162 MPa. Despite the absence of spontaneous fractures in the crowns of the SC and REF cooling protocols, a significant amount of thermal stress is still expected in the structures. In fact, residual stresses in the crowns submitted to the REF protocol seemed to be responsible for their reduced lifetime in the subsequent mechanical test (see section 3.4).

3.3. *Effect of the cooling protocol*

A major source of residual stress in materials that display a viscoelastic behavior through their T_g range is the development of temperature gradients in the structure during the cooling phase [15]. Their occurrence is responsible for an inhomogeneous solidification of the material, creating tensions between the already solidified surfaces and the still viscous inner regions. This becomes critical below the material's T_g, as structural relaxation is hindered by the elastic properties of the solidified glass, resulting in deleterious residual stresses. The magnitude of the temperature gradients in the material and thus, the residual stress developed, is directly related to the applied cooling rate [33]. Accordingly, avoidance of fast cooling regimes around T_g has demonstrated to significantly reduce the development of residual stresses in glassy materials, such as in alumino-silicate glasses used for the veneering of zirconia structures [13,24,25,34]. This has led, in practical terms, to strict firing protocols that reduce temperature gradients in the restorations by keeping the furnace door closed until the temperature drops into a safety range, i.e. below T_g. In the case of Suprinity PC, the manufacturer has set this safety limit at 680 °C. Accordingly, this parameter was considered the "reference" protocol for the crystallization process (REF group) in the current study. The results obtained with the N-type thermocouples for this protocol showed a relatively low cooling rate of 0.4 °C/s at the crown's lumen until 680 °C were reached. However, once the furnace door opened exposing the crowns to the ambient air, a tenfold increase was observed (5.5 °C/s), matching the cooling rate measured for the FC protocol. An even higher cooling rate is expected at the crown's external surfaces, due to the faster dissipation of heat in these regions. On the other hand, temperatures in the SC group decreased at a lower rate (0.4 °C/s) until the furnace door opened at 550 °C.

Aforementioned temperature profiles resulted critical for the development of residual stresses in the structures. As observed in Fig. 7, the highest residual stresses were measured in the FC samples, whereas almost no residual stress development was observed in specimens subjected to the SC protocol. The higher magnitude of residual stress in the transversal section, in contrast to the sagittal slices, is related to the higher

dependency of the hoop component of stress to the cooling regime, as previously observed in zirconia-veneered structures [25]. In addition, a higher stress release during sectioning is expected for this stress component in the sagittal sections, due to its circumferential orientation. Residual stress development in the radial stress component, on the other hand, has shown a higher dependency on the CTE mismatch with a supporting substrate layer [13,25], or, as in the current study, with the firing pin (compare the effect of the firing pin on sagittal and transversal sections of Fig. 4). Thus, the fast cooling protocol caused the outer layers to solidify earlier, contracting at a higher rate than the still hot inner regions. As a consequence, compressive transient stresses developed inside the structure, but were compensated by the low viscosity of the glass melt (still above T_g), which was able to release them. Once solidification took place in the inner regions, the surface had already reached the elastic state, being unable to compensate the internal contraction of the structure, and residual tensile stresses developed here (as observed in the outer rim of the transversal section of the FC sample in Fig. 7). Although the light birefringence method was not capable of determining the nature of the residual stress (i.e. tensile or compressive), development of tensile residual stresses in the surface of fast cooled samples was recently measured by Aurelio et al. [17] using an indentation method. In contrast, application of a slow cooling protocol led to compressive residual stresses in the surface of their samples.

Residual stresses in the REF group had a slightly lower magnitude, although a similar distribution, than the FC samples (Fig. 7). Development of these stresses was probably related to the fast cooling rate of 5.5 °C/s to which the structure was submitted once the furnace opened at 680 °C. A recent thermomechanical analysis (TMA) on this material determined its T_g at 636 °C [30], implying that the transition from the viscous to the solid state did only occurred after exposition of the structure to the ambient air. The cooling rate of crowns in the SC group, on the other hand, was of 0.4 °C/s over the complete T_g range (furnace door opened only at 550 °C), what explains the absence of residual stresses in these samples. In light of the effects of residual stress on the lifetime results displayed in section 3.4, and considering that the SC protocol took only eight minutes longer than the REF protocol, its utilization should be strongly recommended for the crystallization firing of this material.

3.4. *Effect of residual stress on the restoration's lifetime*

The survival analysis of the crowns submitted to chewing simulation is presented in Fig. 8. Only half of the specimens of group 2-REF were able to survive after 10^6 cycles, with two of the crowns developing catastrophic cracks before the first 10^3 cycles were reached. In contrast, no fractures were detected up to 10^5 cycles in specimens crystallized over the fibrous pad (group 4-REF), with a final survival rate for this group of 62.5% after completion of the experiment. The test set up used here for mechanical testing was deliberately designed to challenge the area where residual stresses developed and to study their impact on the restoration's lifetime. Accordingly, obtained results confirmed that the residual stress magnitude around the supporting area of the cordierite pin was high, even in the less aggressive REF cooling protocol. Despite the absence of spontaneous fracture during crystallization (as those observed for FC samples in this group), deleterious tensile stresses were locked inside the restorations and favored the propagation of cracks upon superposition of loading stresses from the chewing simulation. This was confirmed by the fractographic examination of failed crowns of group 2-REF, where all four samples displayed catastrophic cracks in this region. Development of residual stresses in glass-layered zirconia structures has shown to influence the onset [35] and propagation of cracks [14], ultimately leading to partial fractures (or "chippings") in the veneer layer [23]. The lower magnitude of residual stresses in the contact-loading region of crowns of group 4-REF would explain the delayed onset of fractures observed (10^5 cycles). Furthermore, the absence of residual stresses in SC specimens of this group (Fig. 7) correlates well with the superior fatigue performance displayed by these crowns during the chewing simulation (Fig. 8), with a 100% survival rate after 10^6 cycles. These results evidence the relevant role played by residual stresses on the in vitro fatigue response of the restorations, highlighting the advantages of an extended cooling regime for their mechanical performance. To date, only scarce clinical data is available for this material, mainly due to its relatively recent incorporation to the market. Therefore, long-term clinical studies are still needed to assess the clinical relevance of the results presented herein.

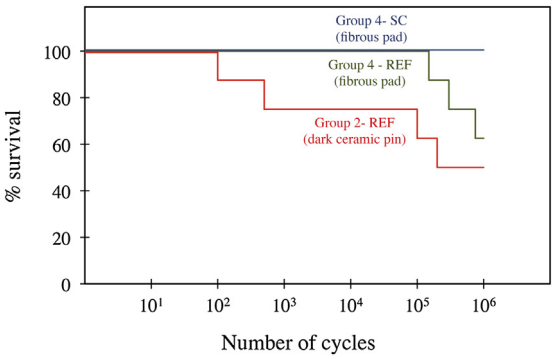

Fig. 8 – Survival analysis of crowns submitted to chewing simulation. All samples of group 4-SC survived after the set interval of 10^6 cycles, whereas only 4 samples of group 2-REF (i.e. 50%) and 5 samples of group 4-REF (i.e. 62.5%) were able to finish the test. However, fracture ensued earlier in group 2-REF (already before 10^3 cycles) than in group 4-REF, where the first fractured crown was detected only after 10^5 cycles.

4. Conclusions

Within the limits of this study, following conclusions can be drawn:

- Residual stresses develop from the direct contact of firing pins with the glass-ceramic, being responsible for an important reduction in the in vitro lifetime of the restorations.

- The use of firing pastes and fibrous pads is able to prevent development of residual stresses in the contact areas between the materials, which favors a better fatigue behavior.
- The use of an extended cooling protocol that ensures a homogenous temperature distribution over the T_g range of the material prevents development of residual stresses and thus, a premature fracture of the crowns.

Acknowledgements

Materials were kindly donated by the manufacturers. This project was supported by Vita Zahnfabrik. The Suprinity PC crowns for the chewing simulation experiment were CAD/CAM milled at Vita Zahnfabrik. We especially thank H. Katte from ilis GmbH for his support and discussions regarding the birefringence measurements.

REFERENCES

[1] Lien W, Roberts HW, Platt JA, Vandewalle KS, Hill TJ, Chu T-MG. Microstructural evolution and physical behavior of a lithium disilicate glass–ceramic. Dent Mater 2015;31:928–40.
[2] Belli R, Wendler M, Cicconi MR, de Ligny D, Petschelt A, Werbach K, et al. Fracture anisotropy in texturized lithium disilicate glass-ceramics. J Non Cryst Solids 2018;481:457–69.
[3] Hurle K, Belli R, Götz-Neunhoeffer F, Lohbauer U. Phase characterization of lithium silicate biomedical glass-ceramics produced by two-stage crystallization. J Non Cryst Solids 2019;510:42–50.
[4] Krüger S, Deubener J, Ritzberger C, Höland W. Nucleation kinetics of lithium metasilicate in ZrO_2-bearing lithium disilicate glasses for dental application. Int J Appl Glass Sci 2013;4:9–19.
[5] Belli R, Wendler M, de Ligny D, Cicconi MR, Petschelt A, Peterlik H, et al. Chairside CAD/CAM materials. Part 1: measurement of elastic constants and microstructural characterization. Dent Mater 2017;33:84–98.
[6] Elsaka SE. Optical and mechanical properties of newly developed monolithic multilayer zirconia. J Prosthodont 2019;28:e279–84.
[7] Schwindling FS, Rues S, Schmitter M. Fracture resistance of glazed, full-contour ZLS incisor crowns. J Prosthodont Res 2017;61:344–9.
[8] Sieper K, Wille S, Kern M. Fracture strength of lithium disilicate crowns compared to polymer-infiltrated ceramic-network and zirconia reinforced lithium silicate crowns. J Mech Behav Biomed Mater 2017;74:342–8.
[9] Springall GAC, Yin L. Nano-scale mechanical behavior of pre-crystallized CAD/CAM zirconia-reinforced lithium silicate glass ceramic. J Mech Behav Biomed Mater 2018;82:35–44.
[10] Serbena FC, Zanotto ED. Internal residual stresses in glass-ceramics: a review. J Non Cryst Solids 2012;358:975–84.
[11] Denry IL, Holloway JA. Effect of post-processing heat treatment on the fracture strength of a heat-pressed dental ceramic. J Biomed Mater Res B Appl Biomater 2004;68B:174–9.
[12] Lohbauer U, Scherrer SS, Della Bona A, Tholey M, van Noort R, Vichi A, et al. ADM guidance-ceramics: all-ceramic multilayer interfaces in dentistry. Dent Mater 2017;33:585–98.
[13] Belli R, Monteiro Jr S, Baratieri L, Katte H, Petschelt A, Lohbauer U. A photoelastic assesment of residual stresses in zirconia-veneer crowns. J Dent Res 2012;91:316–20.
[14] Wendler M, Belli R, Petschelt A, Lohbauer U. Characterization of residual stresses in zirconia veneered bilayers assessed via sharp and blunt indentation. Dent Mater 2015;31:948–57.
[15] Swain M. Unstable cracking (chipping) of veneering porcelain on all-ceramic dental crowns and fixed partial dentures. Acta Biomater 2009;5:1668–77.
[16] Al-Amleh B, Neil Waddell J, Lyons K, Swain MV. Influence of veneering porcelain thickness and cooling rate on residual stresses in zirconia molar crowns. Dent Mater 2014;30:271–80.
[17] Aurelio IL, Dorneles LS, May LG. Extended glaze firing on ceramics for hard machining: crack healing, residual stresses, optical and microstructural aspects. Dent Mater 2017;33:226–40.
[18] Li D, Li XC, Zhang ZZ, Zhang SF, He L. Understanding the mechanism for the mechanical property degradation of a lithium disilicate glass-ceramic by annealing. J Mech Behav Biomed Mater 2018;78:28–35.
[19] Katte H. Imaging measurements of stress birefringence in optical materials and components. Photonik Int 2009;1:39–41.
[20] Durelli A, Riley W. Introduction to photomechanics. Englewood Cliffs, NJ, USA: Prentice-Hall; 1965.
[21] Baldassarri M, Stappert C, Wolff M, Thompson V, Zhang Y. Residual stresses in porcelain-veneered zirconia prostheses. Dent Mater 2012;28:873–9.
[22] Aboushelib M, Feilzer A, de Jager N, Kleverlaan C. Prestresses in bilayered all-ceramic restorations. J Biomed Mater Res B Appl Biomater 2008;87:139–45.
[23] Belli R, Frankenberger R, Appelt A, Schmitt J, Baratieri L, Greil P, et al. Thermal-induced residual stresses affect the lifetime of zirconia-veneer crowns. Dent Mater 2013;29:181–90.
[24] Tholey M, Swain M, Thiel N. Thermal gradients and residual stresses in veneered Y-TZP frameworks. Dent Mater 2011;27:1102–10.
[25] Wendler M, Belli R, Petschelt A, Lohbauer U. Spatial distribution of residual stresses in glass-ZrO_2 sphero-cylindrical bilayers. J Mech Behav Biomed Mater 2016;60:535–46.
[26] Vita-Zahnfabrik. Vita Suprinity PC. Working instructions. v007. URL: https://mam.vita-zahnfabrik.com/portal/ecms_mdb_download.php?id=82430&sprache=en&fallback=de&rechtsraum=&cls_session_id=&neuste_version=1. 2019.
[27] Kuscer D, Bantan I, Hrovat M, Malič B. The microstructure, coefficient of thermal expansion and flexural strength of cordierite ceramics prepared from alumina with different particle sizes. J Eur Ceram Soc 2017;37:739–46.
[28] Peterson IM, Tien T-Y. Effect of the grain boundary thermal expansion coefficient on the fracture toughness in silicon nitride. J Am Ceram Soc 1995;78:2345–52.
[29] Kirby RK. Platinum—a thermal expansion reference material. Int J Thermophys 1991;12:679–85.
[30] Lohbauer U, Wendler M, Rapp D, Belli R. Fractographic analysis of lithium silicate crown failures during sintering. SAGE Open Med Case Rep 2019;7:1–8, http://dx.doi.org/10.1177/2050313X19838962.
[31] Quinn G. Fractography of ceramics and glasses—practice guide. NIST; 2016.
[32] Belli R, Wendler M, Petschelt A, Lube T, Lohbauer U. Fracture toughness testing of biomedical ceramic-based materials using beams, plates and discs. J Eur Ceram Soc 2018;38:5533–44.
[33] Taskonak B, Borges G, Melcholsky Jr J, Anusavice K, Moore B, Yan J. The effects of viscoelastic parameters on residual

stress development in a zirconia/glass bilayer dental ceramic. Dent Mater 2008;24:1149–55.
[34] Benetti P, Kelly JR, Sanchez M, Della Bona A. Influence of thermal gradients on stress state of veneered restorations. Dent Mater 2014;30:554–63.
[35] Zhang Z, Guazzato M, Sornsuwan T, Scherrer S, Rungsiyakull C, Li W, et al. Thermally induced fracture for core-veneered dental ceramic structures. Acta Biomater 2013;9:8394–402.